



Searching for axion-like particles at future e^+e^- and e^-p colliders

Han Wang (王晗)

Liaoning Normal University

27th Mini-workshop on the frontier of LHC

2024.01.22

Based on Phys.Lett.B 848 (2024) 138368 with **C.-X. Yue** and **Y.-Q. Wang**

Phys.Rev.D 107 (2023) 11, 115025 with **C.-X. Yue**, **X.-J Cheng** and **Y.-Q. Wang**

J.Phys.G 49 (2022) 11, 115002 with **C.-X. Yue**, **Y.-C. Guo**, **X.-J Cheng** and **X.-Y. Li**

Outline

1

Introduction

2

Searching for axion-like particles at the CEPC via the triphoton channel

3

Sensitivity of the future $e^- p$ collider to the coupling of axion-like particles with W^\pm bosons

4

Detecting the coupling of axion-like particles with fermions at the ILC

5

Conclusions

1.1 Properties of axion-like particles (ALPs)

- generalizations of QCD axions
 - CP-odd neutral pseudoscalars
 - the masses
 - couplings to the SM particles
- singlets
- independent parameters

1.2 Effective interactions of ALP

The effective interactions of ALP with the SM particles:

$$\mathcal{L}_{eff} = \frac{1}{2}(\partial^\mu a)(\partial_\mu a) - \frac{1}{2}m_a^2 a^2 + \frac{\partial^\mu a}{f_a} \sum_{\psi=Q_L, Q_R, L_L, L_R} \bar{\psi} \gamma_\mu X_\psi \psi - C_{\tilde{B}} \frac{a}{f_a} B_{\mu\nu} \tilde{B}^{\mu\nu} - C_{\tilde{W}} \frac{a}{f_a} W_{\mu\nu}^i \tilde{W}^{i\mu\nu}$$

m_a : the mass of ALP

f_a : the characteristic scale

$W_{\mu\nu}^i$ and $B_{\mu\nu}$: the field strength tensors of $SU(2)_L$ and $U(1)_Y$

$C_{\tilde{W}}$ and $C_{\tilde{B}}$: the coupling constants

X_ψ : Hermitian matrices in flavour space

1 Introduction

After electroweak symmetry breaking:

$$\begin{aligned}\mathcal{L}_{eff} = & \frac{1}{2}(\partial^\mu a)(\partial_\mu a) - \frac{1}{2}m_a^2 a^2 + ig_{a\psi} a \sum_{\psi=Q,L} m_\psi^{diag} \bar{\psi} \gamma_5 \psi \\ & - \frac{1}{4}g_{a\gamma} a F_{\mu\nu} \tilde{F}^{\mu\nu} - \frac{1}{4}g_{aZ} a Z_{\mu\nu} \tilde{Z}^{\mu\nu} - \frac{1}{4}g_{a\gamma Z} a F_{\mu\nu} \tilde{Z}^{\mu\nu} - \frac{1}{4}g_{aWW} a W_{\mu\nu} \tilde{W}^{\mu\nu}\end{aligned}$$

m_ψ^{diag} : the diagonalizable fermion mass matrix

$F_{\mu\nu}$: the photon field strength tensor

$Z_{\mu\nu}$: the Z boson field strength tensor

$W_{\mu\nu}$: the W boson field strength tensor

1 Introduction



all the couplings $g_{a\gamma\gamma}$, g_{aZZ} , $g_{aZ\gamma}$, g_{aWW} and $g_{a\psi}$ are governed by f_a

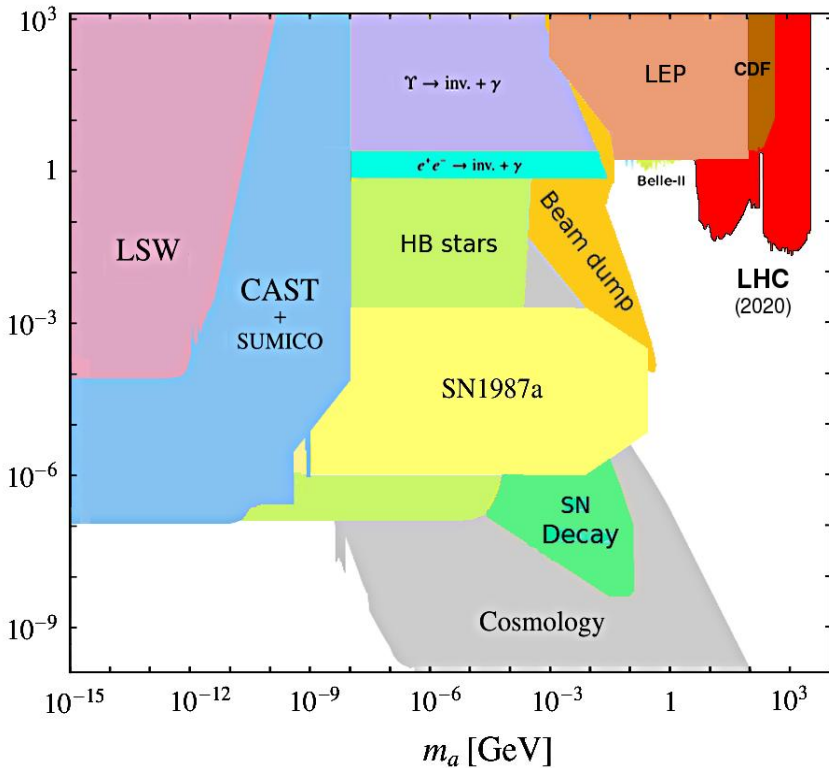
where

$$g_{a\gamma\gamma} = \frac{4}{f_a} (c_W^2 C_{\tilde{B}} + s_W^2 C_{\tilde{W}}), \quad g_{aZZ} = \frac{4}{f_a} (s_W^2 C_{\tilde{B}} + c_W^2 C_{\tilde{W}}),$$
$$g_{a\gamma Z} = \frac{8}{f_a} s_W c_W (C_{\tilde{W}} - C_{\tilde{B}}), \quad g_{aWW} = \frac{4}{f_a} C_{\tilde{W}}$$

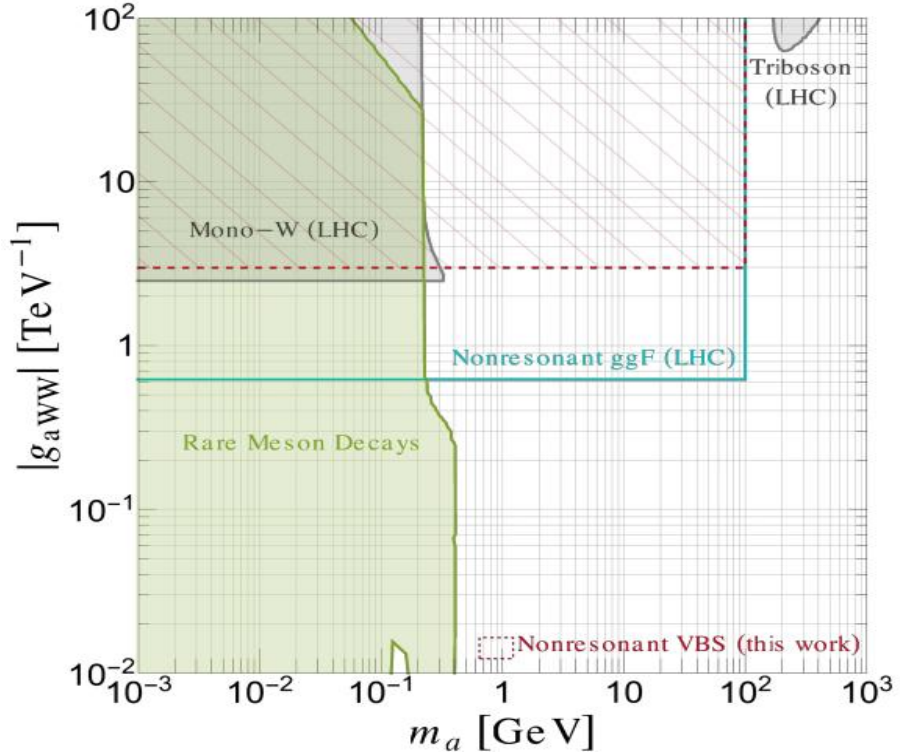
s_W and c_W : the sine and cosine of the weak mixing angle

1.3 The constraints on the effective couplings of ALP to the SM bosons or fermions

D. d'Enterria, in *Workshop on Feebly Interacting Particles* (2021), 2102.08971



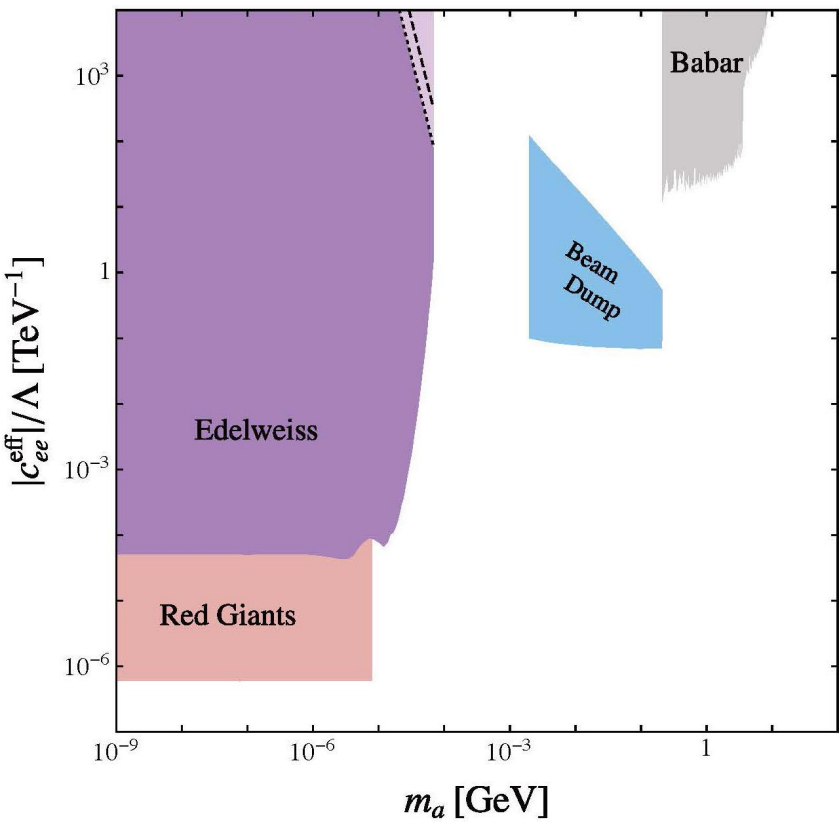
J. Bonilla, I. Brivio, J. Machado-Rodríguez, and J. F. de Trocóniz,
JHEP **06**, 113 (2022), 2202.03450



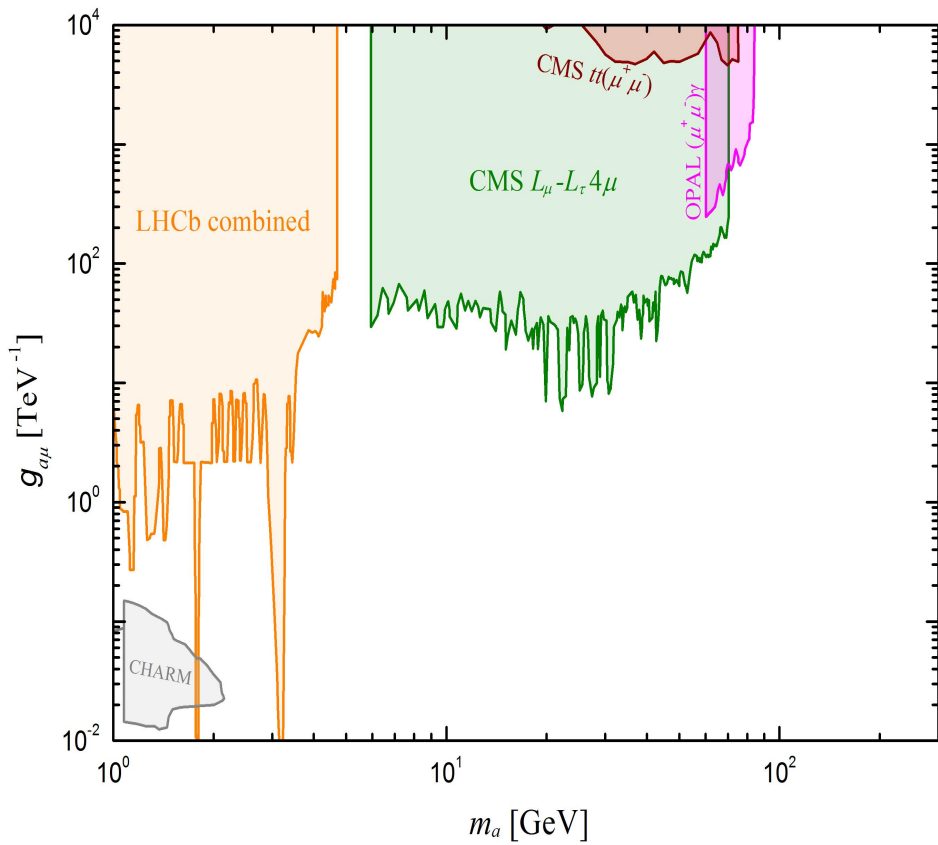
Existing constraints on the ALP–photon coupling (left) and ALP– W^\pm coupling (right)

1.3 The constraints on the effective couplings of ALP to the SM bosons or fermions

M. Bauer, M. Neubert, and A. Thamm, JHEP **12**, 044 (2017), 1708.00443



J. Liu, X. Ma, L.-T. Wang, and X.-P. Wang,
Phys. Rev. D **107**, 095016 (2023), 2210.09335



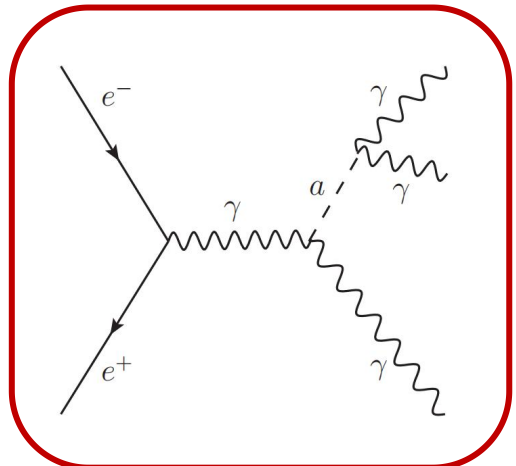
Existing constraints on the ALP–electron coupling (left) and ALP–muon coupling (right)



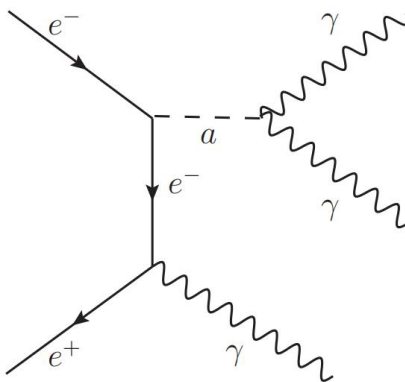
J.Phys.G 49 (2022) 11, 115002

Han Wang, Chong-Xing Yue*,
Yu-Chen Guo, Xue-Jia Cheng
and Xin-Yang Li

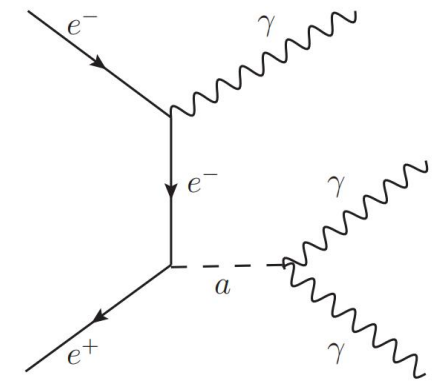
- $C_{\tilde{W}} = C_{\tilde{B}}$ $\longrightarrow g_{a\gamma\gamma} = g_{aZZ} = g_{aWW}$ and $g_{a\gamma Z} = 0$
- The Feynman diagrams for the process of $e^+e^- \rightarrow a\gamma \rightarrow 3\gamma$



(a)



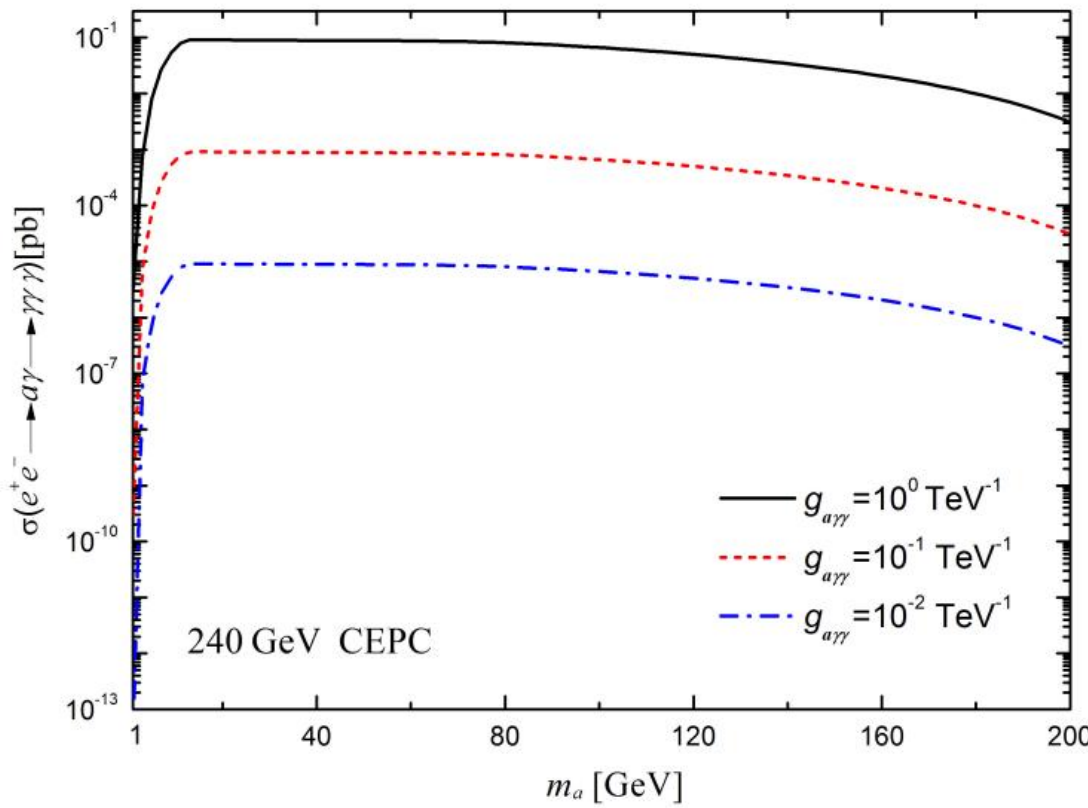
(b)



(c)

dominant

- CEPC $E_{CM} = 240 \text{ GeV}$ $\mathcal{L} = 5.6 \text{ ab}^{-1}$ $1 \text{ GeV} < m_a \leq 200 \text{ GeV}$
- The cross section of the process $e^+e^- \rightarrow a\gamma \rightarrow 3\gamma$ as a function of the ALP mass m_a



- Basic cuts:

$$p_T^\gamma > 10 \text{ GeV}$$

$$|\eta_\gamma| < 2.5$$

$$\Delta R_{\gamma\gamma} > 0.2 \quad (\Delta R = \sqrt{(\Delta\phi)^2 + (\Delta\eta)^2})$$

Tools added:

MLAnalysis <https://github.com/NBAlexis/MLAnalysis>

- The angular separation of the two photons from ALP decay strongly depends on the ALP mass

- $m_a \leq 20 \text{ GeV}$  $N_\gamma \geq 1$

the invariant mass of
all final state photons m_γ

observables

the transverse momentum of
the hardest photon in the final states $p_T^{\gamma_1}$

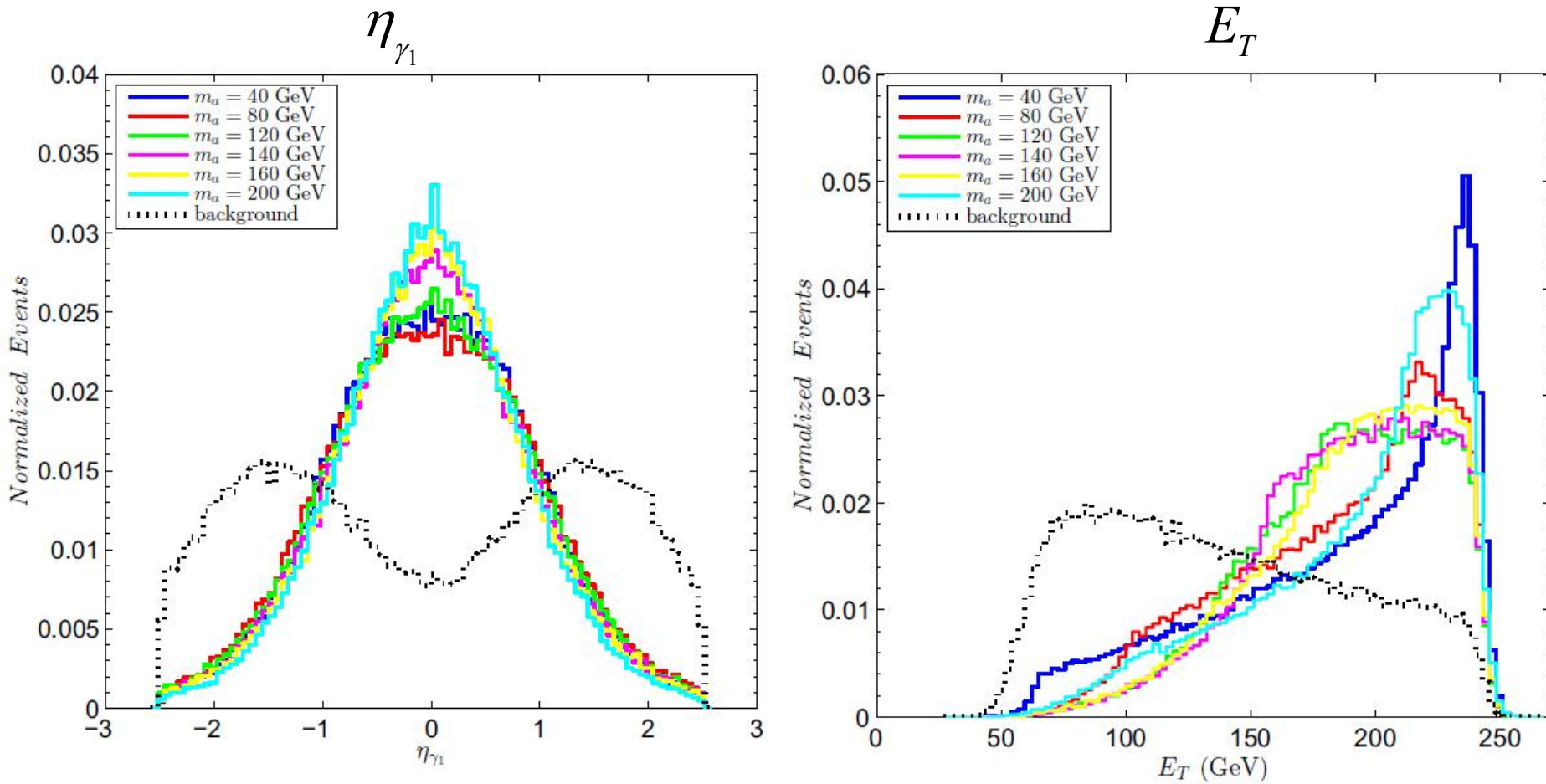
- $m_a > 20 \text{ GeV}$  $N_\gamma \geq 3$

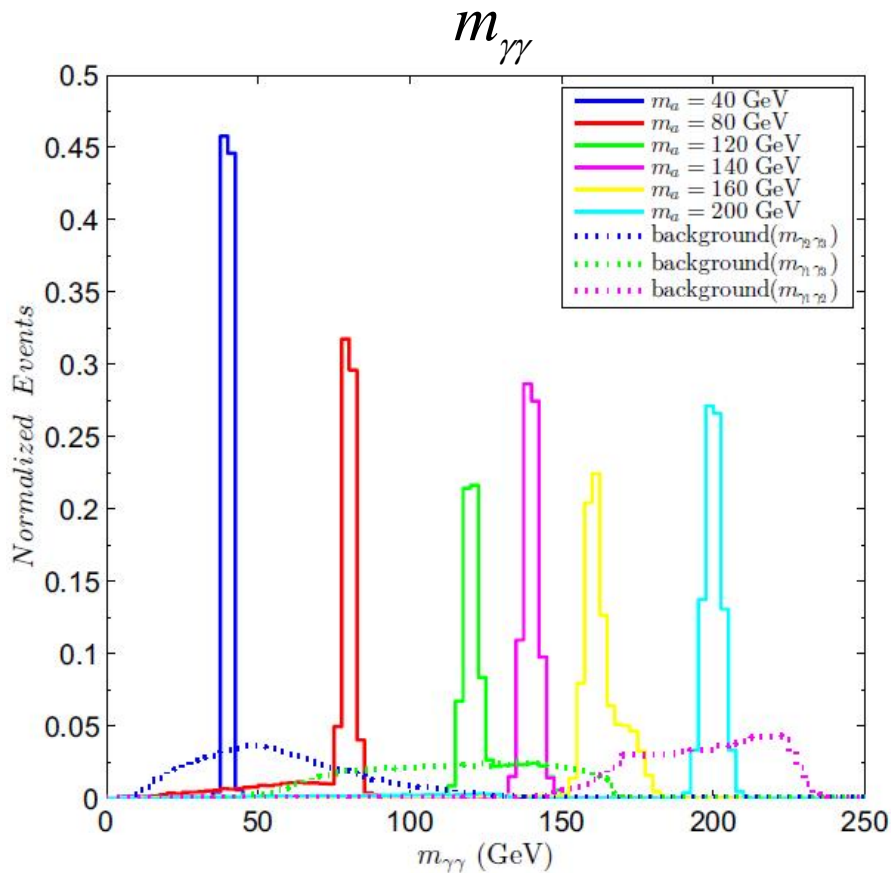
η_{γ_1}

E_T

$m_{\gamma\gamma}$

 observables





- The symbols γ_1, γ_2 and γ_3 :

The photons with the largest,
intermediate and smallest momentum

- high mass ALP $\rightarrow \gamma_1\gamma_2$

- low mass ALP $\rightarrow \gamma_2\gamma_3$



- The improved cuts

Cut \ mass	$1 \text{ GeV} < m_a \leq 20 \text{ GeV}$	$20 \text{ GeV} < m_a \leq 200 \text{ GeV}$
Cut1	$N_\gamma \geq 1$	$N_\gamma \geq 3$
Cut2	$m_\gamma \leq 20 \text{ GeV}$	$ \eta_{\gamma_1} < 1.7$
Cut3	$p_T^{\gamma_1} \geq 20 \text{ GeV}$	$E_T \geq 100 \text{ GeV}$
Cut4	—	$ m_{\gamma\gamma} - m_a \leq 5 \text{ GeV}$

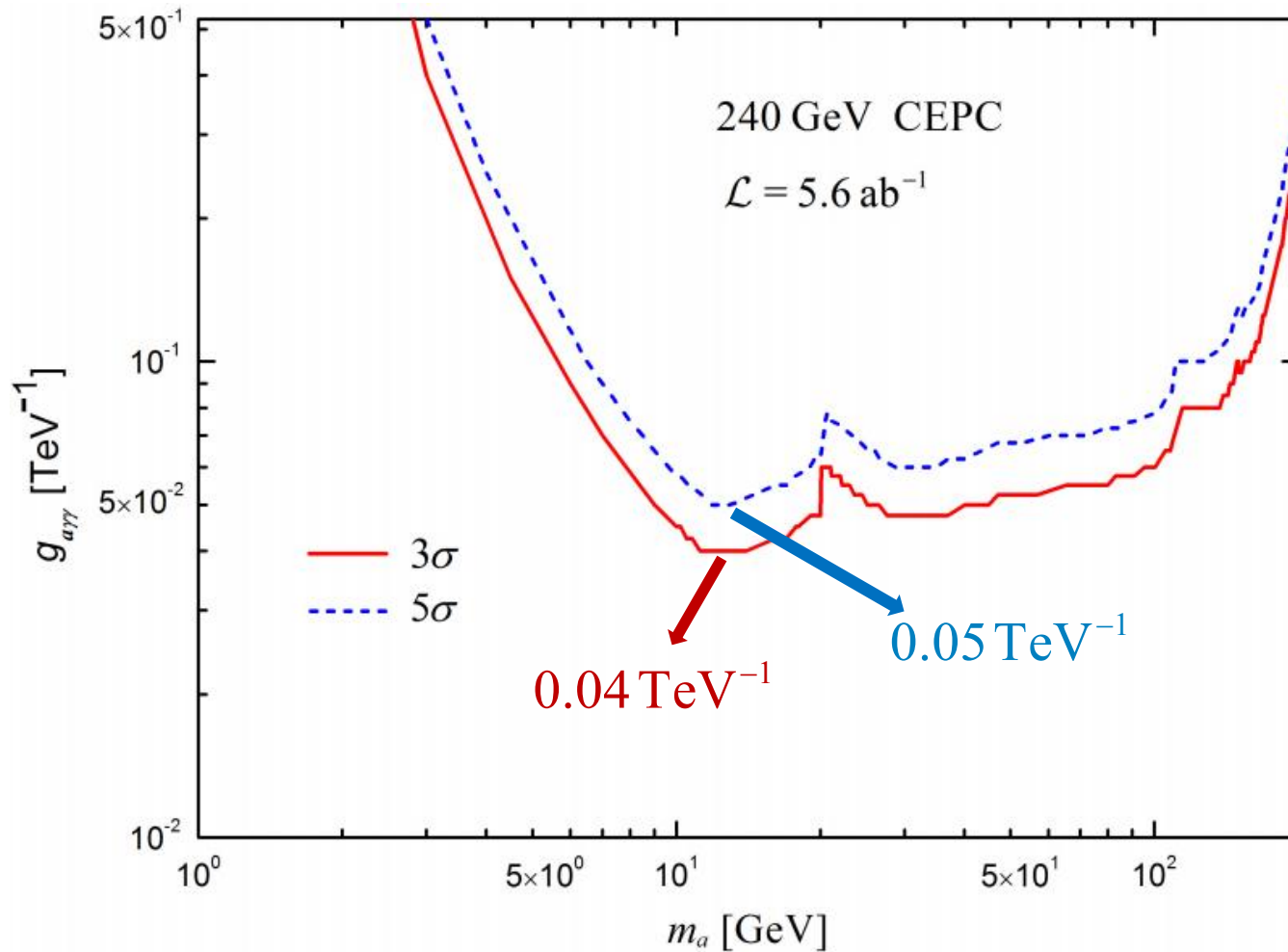


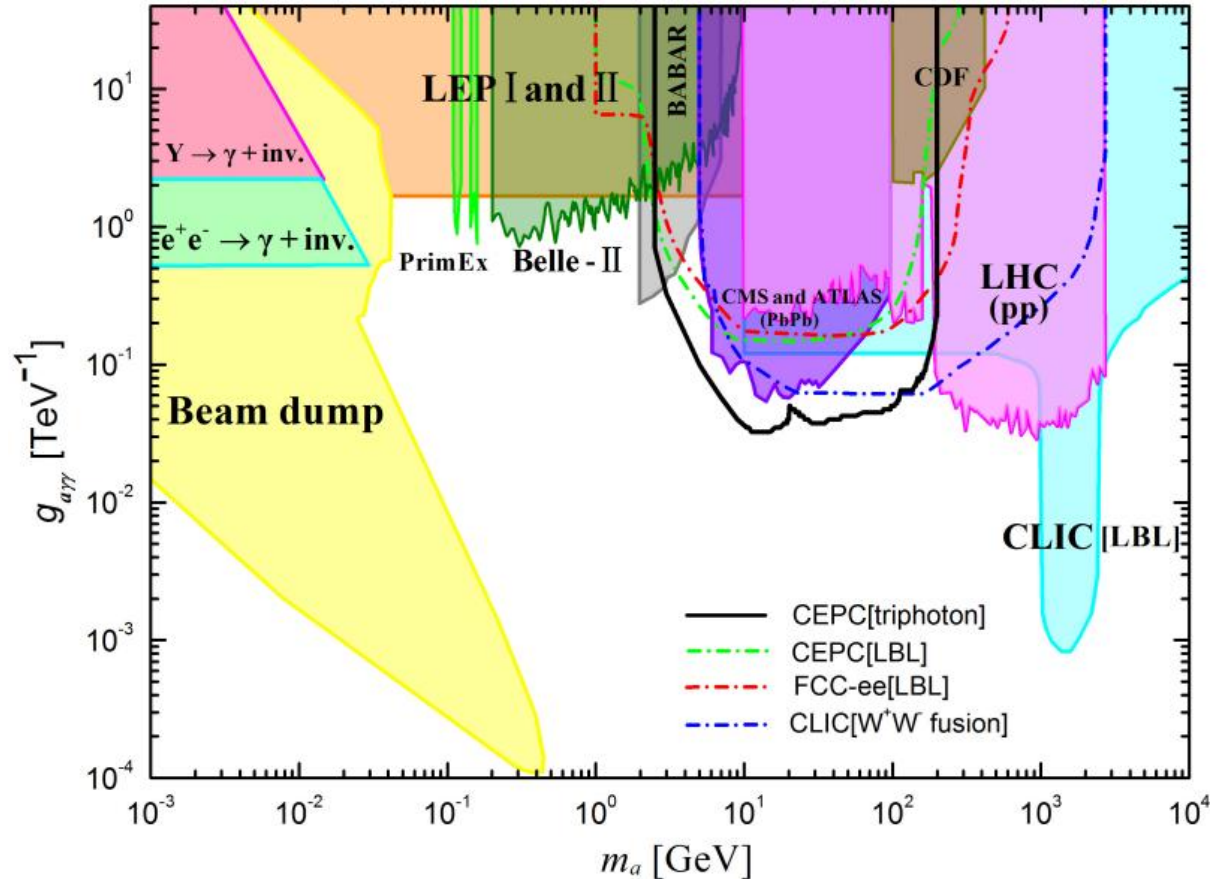
m_a [GeV]	cross sections for signal(background)[pb]					SS
	Basic Cuts	Cut1	Cut2	Cut3	Cut4	
10	6.5893×10^{-4} (0.2851)	6.5303×10^{-4} (0.2850)	5.8278×10^{-4} (0.0087)	5.8259×10^{-4} (0.0086)	—	14.38
20	9.0768×10^{-4} (0.2851)	9.0260×10^{-4} (0.2850)	4.9382×10^{-4} (0.0087)	4.9369×10^{-4} (0.0086)	—	12.24
40	8.9170×10^{-4} (0.2851)	8.1998×10^{-4} (0.2679)	7.7072×10^{-4} (0.1842)	7.5997×10^{-4} (0.1739)	7.5569×10^{-4} (0.0202)	12.35
80	8.0760×10^{-4} (0.2851)	7.3533×10^{-4} (0.2679)	6.8321×10^{-4} (0.1842)	6.7924×10^{-4} (0.1739)	5.4713×10^{-4} (0.0178)	9.56
120	5.0300×10^{-4} (0.2851)	4.5322×10^{-4} (0.2679)	4.2267×10^{-4} (0.1842)	4.2141×10^{-4} (0.1739)	2.8405×10^{-4} (0.0189)	4.85
140	3.4438×10^{-4} (0.2851)	3.0861×10^{-4} (0.2679)	2.8993×10^{-4} (0.1842)	2.8918×10^{-4} (0.1739)	2.5867×10^{-4} (0.0204)	4.26
160	2.0613×10^{-4} (0.2851)	1.8364×10^{-4} (0.2679)	1.7283×10^{-4} (0.1842)	1.7234×10^{-4} (0.1739)	1.2056×10^{-4} (0.0103)	2.80
200	3.0873×10^{-5} (0.2851)	2.7060×10^{-5} (0.2679)	2.5737×10^{-5} (0.1842)	2.5585×10^{-5} (0.1739)	2.3273×10^{-5} (0.0251)	0.35

- $g_{a\gamma\gamma} = 10^{-4} \text{ GeV}^{-1}$



- The 3σ and 5σ curves for the process $e^+e^- \rightarrow a\gamma \rightarrow 3\gamma$ in the $(m_a, g_{a\gamma\gamma})$ plane



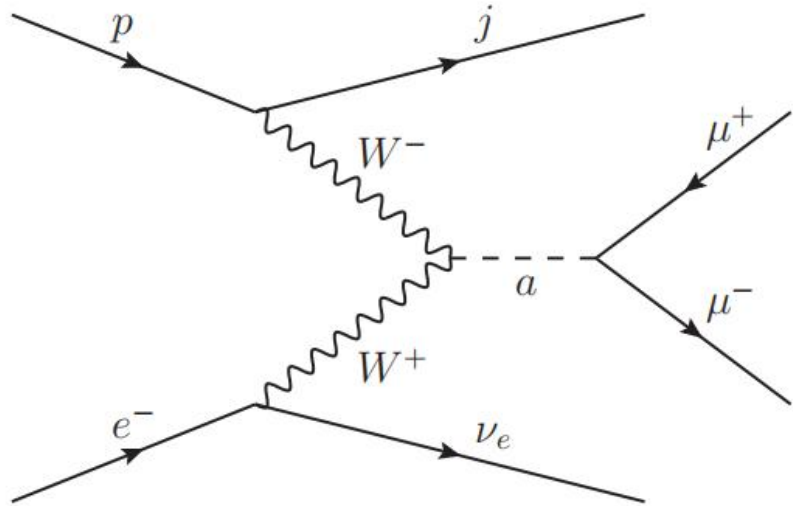


- The promising sensitivities as $g_{a\gamma\gamma} \in [0.0325, 0.37] \text{ TeV}^{-1}$ with $m_a \in [2.9, 190] \text{ GeV}$ at 2σ level

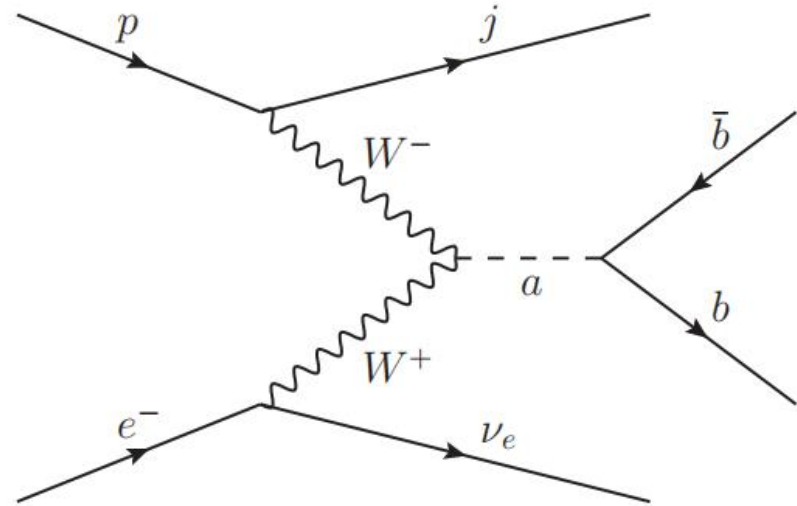


Phys.Rev.D 107 (2023) 11, 115025

**Chong-Xing Yue, Han Wang*,
Xue-Jia Cheng and Yue-Qi Wang**

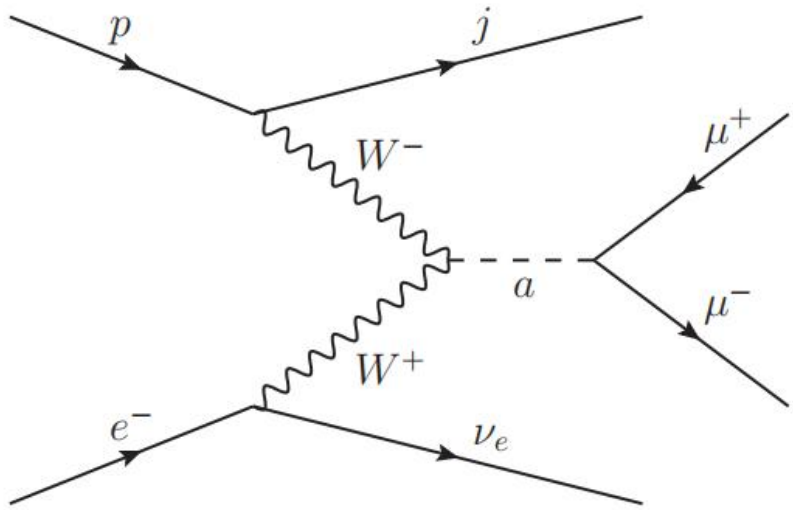


$$e^- p \rightarrow \nu_e ja(a \rightarrow \mu^+ \mu^-)$$



$$e^- p \rightarrow \nu_e ja(a \rightarrow b\bar{b})$$

Searching for ALP via $e^- p \rightarrow \nu_e j a (a \rightarrow \mu^+ \mu^-)$



-

LHeC

$$E_{CM} = 1.3 \text{ TeV}$$

$$\mathcal{L} = 1 \text{ ab}^{-1}$$

- $5 \text{ GeV} \leq m_a \leq 1000 \text{ GeV}$
- Basic cuts:

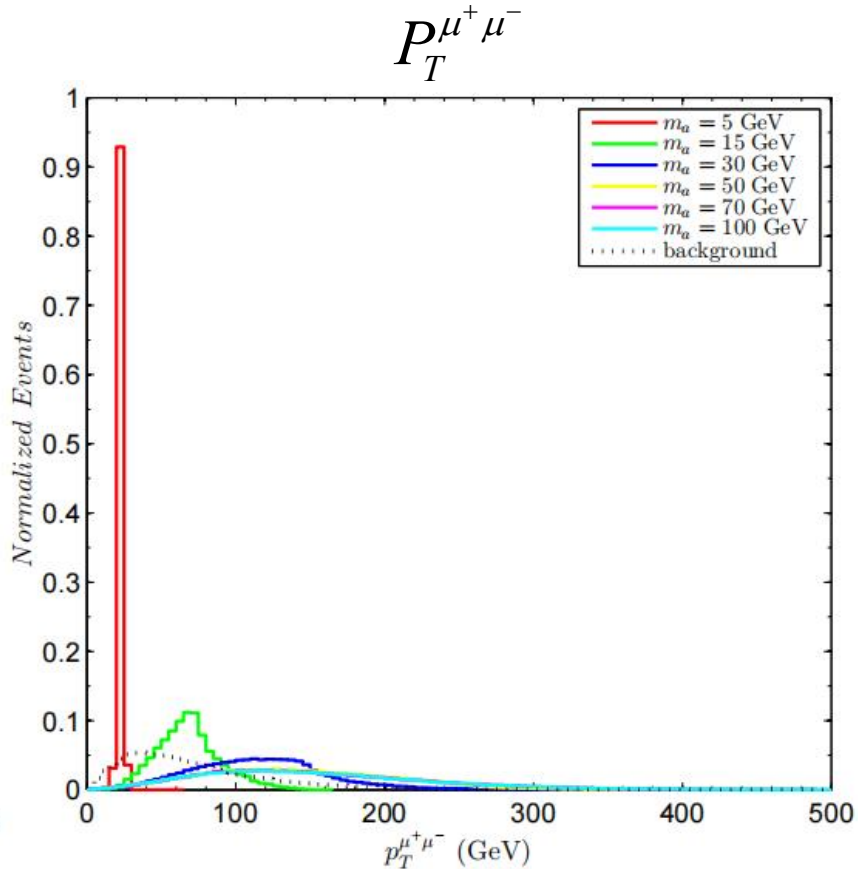
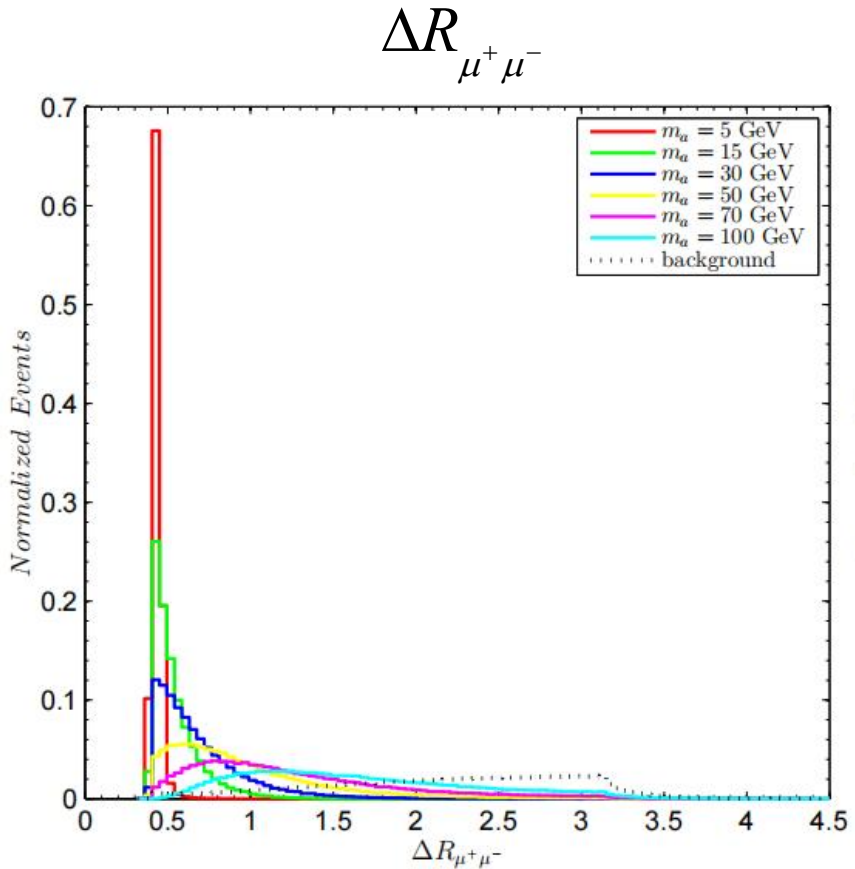
$$P_T^l > 10 \text{ GeV}$$

$$P_T^j > 20 \text{ GeV}$$

$$|\eta_l| < 2.5 \quad |\eta_j| < 5$$

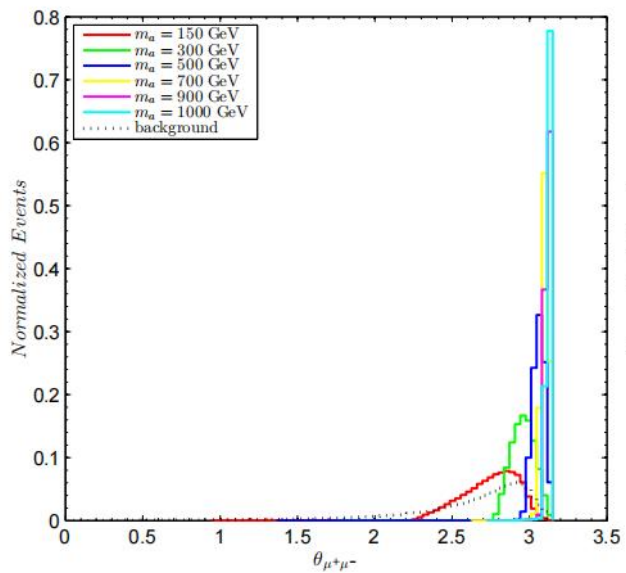
$$\Delta R_{ll} > 0.4 \quad \Delta R_{jj} > 0.4 \quad \Delta R_{lj} > 0.4$$

- $5 \text{ GeV} \leq m_a \leq 100 \text{ GeV}$

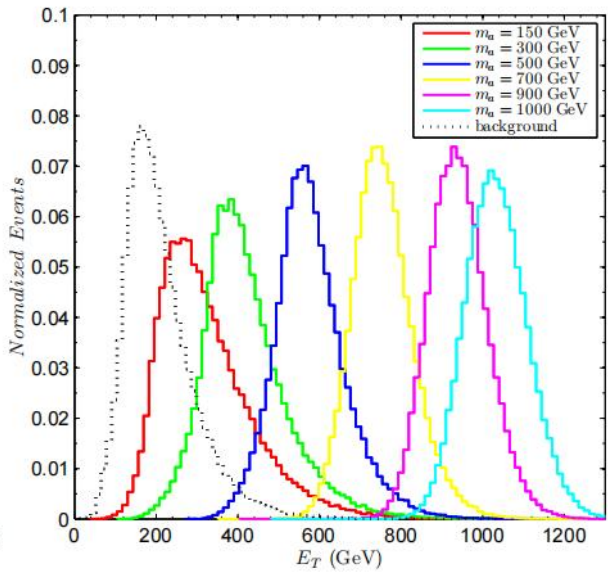


- $100 \text{ GeV} < m_a \leq 1000 \text{ GeV}$

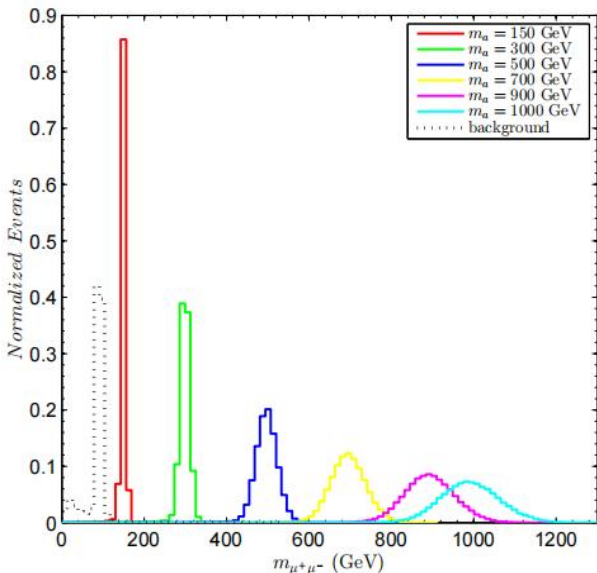
$\theta_{\mu^+\mu^-}$



E_T



$m_{\mu^+\mu^-}$





- The improved cuts

Cuts	Mass	
	$5 \text{ GeV} \leq m_a \leq 100 \text{ GeV}$	$100 \text{ GeV} < m_a \leq 1000 \text{ GeV}$
Cut 1	$N_{\mu^+} \geq 1, N_{\mu^-} \geq 1, N_j \geq 1$	$N_{\mu^+} \geq 1, N_{\mu^-} \geq 1, N_j \geq 1$
Cut 2	$\Delta R_{\mu^+\mu^-} < 1.8$	$\theta_{\mu^+\mu^-} > 2.1$
Cut 3	$p_T^{\mu^+\mu^-} > 20 \text{ GeV}$	$E_T > 250 \text{ GeV}$
Cut 4	—	$m_{\mu^+\mu^-} > 100 \text{ GeV}$

Sensitivity of the future e^-p collider to the coupling of axion-like particles with W^\pm bosons

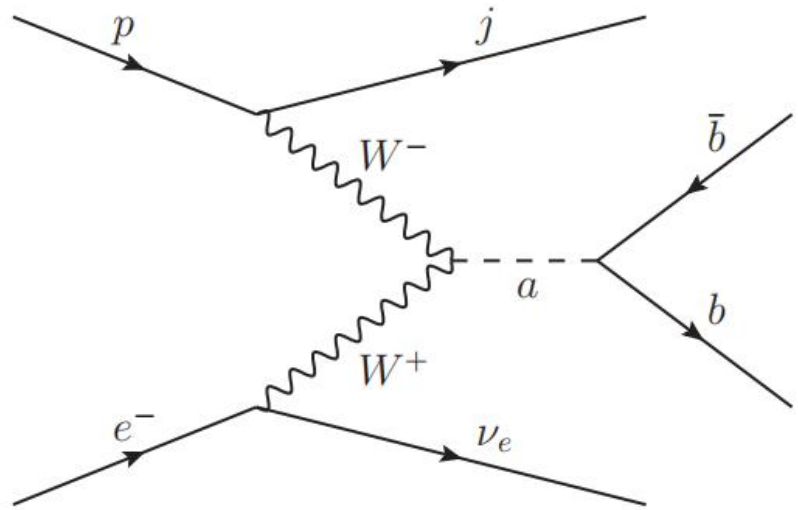


Cuts	cross sections for signal (background) [pb]					
	$m_a = 5 \text{ GeV}$	$m_a = 15 \text{ GeV}$	$m_a = 30 \text{ GeV}$	$m_a = 50 \text{ GeV}$	$m_a = 70 \text{ GeV}$	$m_a = 100 \text{ GeV}$
Basic Cuts	1.7442×10^{-6} (0.0142)	5.2885×10^{-4} (0.0142)	2.0437×10^{-3} (0.0142)	2.8861×10^{-3} (0.0142)	2.9864×10^{-3} (0.0142)	2.7399×10^{-3} (0.0142)
	1.4435×10^{-6} (0.0128)	4.6473×10^{-4} (0.0128)	1.8361×10^{-3} (0.0128)	2.6165×10^{-3} (0.0128)	2.7072×10^{-3} (0.0128)	2.4812×10^{-3} (0.0128)
Cut 1	1.4435×10^{-6} (3.9212×10^{-3})	4.6463×10^{-4} (3.9212×10^{-3})	1.8156×10^{-3} (3.9212×10^{-3})	2.4350×10^{-3} (3.9212×10^{-3})	2.2205×10^{-3} (3.9212×10^{-3})	1.5666×10^{-3} (3.9212×10^{-3})
	1.3934×10^{-6} (3.8963×10^{-3})	4.6375×10^{-4} (3.8963×10^{-3})	1.8155×10^{-3} (3.8963×10^{-3})	2.4349×10^{-3} (3.8963×10^{-3})	2.2205×10^{-3} (3.8963×10^{-3})	1.5666×10^{-3} (3.8963×10^{-3})
Cut 2						
Cut 3						
SS	0.022	7.015	24.022	30.609	28.396	21.196

Cuts	cross sections for signal (background) [pb]					
	$m_a = 150 \text{ GeV}$	$m_a = 300 \text{ GeV}$	$m_a = 500 \text{ GeV}$	$m_a = 700 \text{ GeV}$	$m_a = 900 \text{ GeV}$	$m_a = 1000 \text{ GeV}$
Basic Cuts	2.1509×10^{-3} (0.0142)	8.8581×10^{-4} (0.0142)	2.0197×10^{-4} (0.0142)	2.7954×10^{-5} (0.0142)	1.5617×10^{-6} (0.0142)	1.9118×10^{-7} (0.0142)
	1.9429×10^{-3} (0.0128)	7.9889×10^{-4} (0.0128)	1.8218×10^{-4} (0.0128)	2.4999×10^{-5} (0.0128)	1.3965×10^{-6} (0.0128)	1.7116×10^{-7} (0.0128)
Cut 1	1.9417×10^{-3} (0.0112)	7.9882×10^{-4} (0.0112)	1.8218×10^{-4} (0.0112)	2.4999×10^{-5} (0.0112)	1.3965×10^{-6} (0.0112)	1.7116×10^{-7} (0.0112)
	1.3790×10^{-3} (3.2070×10^{-3})	7.7811×10^{-4} (3.2070×10^{-3})	1.8218×10^{-4} (3.2070×10^{-3})	2.4999×10^{-5} (3.2070×10^{-3})	1.3965×10^{-6} (3.2070×10^{-3})	1.7116×10^{-7} (3.2070×10^{-3})
Cut 2	1.3713×10^{-3} (2.2571×10^{-4})	7.7691×10^{-4} (2.2571×10^{-4})	1.8208×10^{-4} (2.2571×10^{-4})	2.4989×10^{-5} (2.2571×10^{-4})	1.3965×10^{-6} (2.2571×10^{-4})	1.7116×10^{-7} (2.2571×10^{-4})
Cut 3						
Cut 4						
SS	34.309	24.526	8.986	1.581	0.093	0.011

- $g_{aWW} = 1 \text{ TeV}^{-1}$

Searching for ALP via $e^- p \rightarrow \nu_e j a (a \rightarrow b\bar{b})$

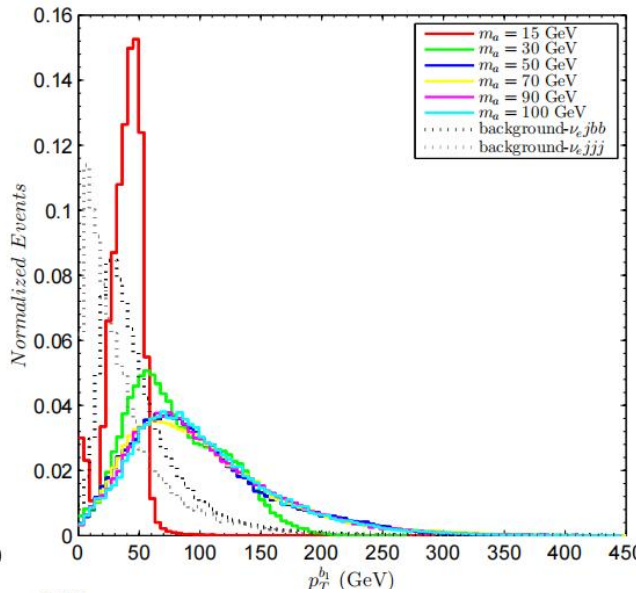
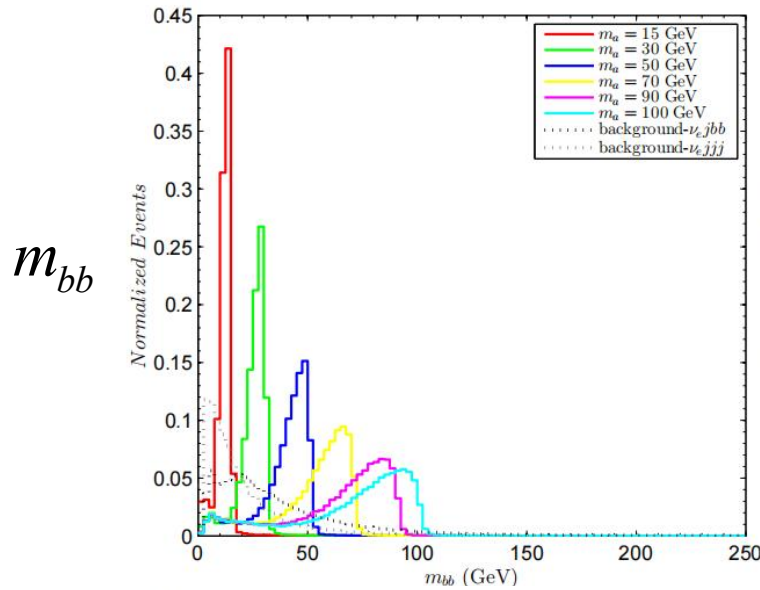


- $E_{CM} = 1.3 \text{ TeV}$
- $\mathcal{L} = 1 \text{ ab}^{-1}$
- $15 \text{ GeV} \leq m_a \leq 1000 \text{ GeV}$
- Basic cuts:
 - $P_T^l > 10 \text{ GeV}$
 - $P_T^j > 20 \text{ GeV}$
 - $|\eta_l| < 2.5$
 - $|\eta_j| < 5$

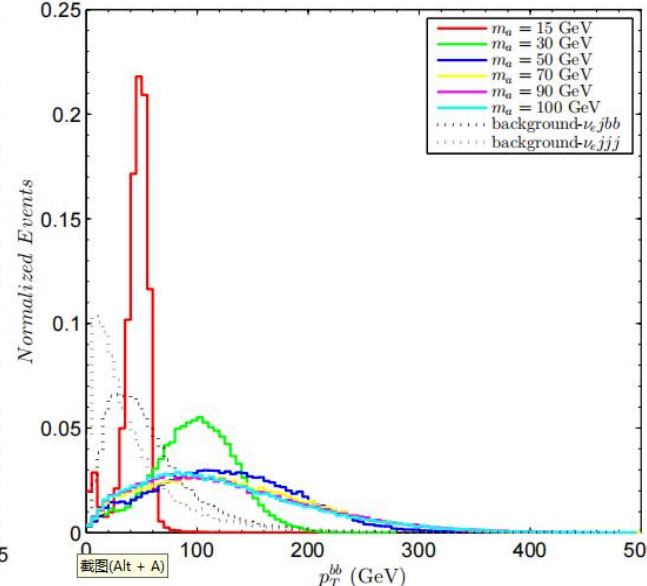
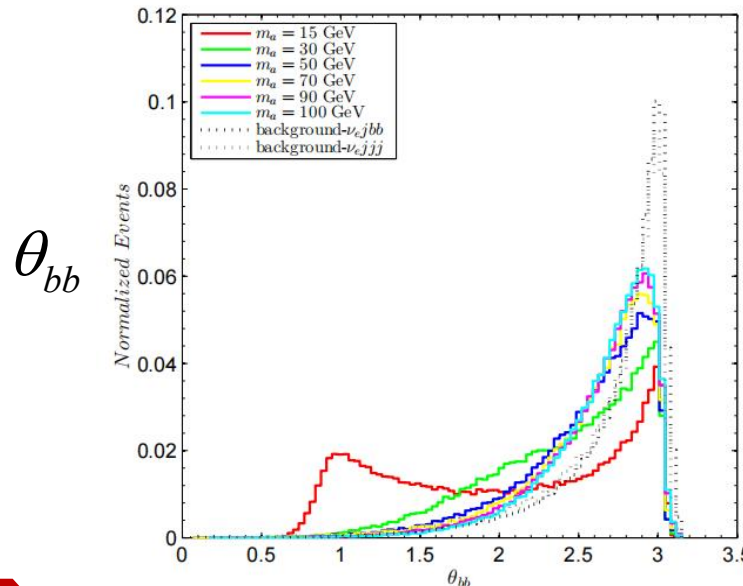
$$\Delta R_{ll} > 0.4 \quad \Delta R_{jj} > 0.4 \quad \Delta R_{lj} > 0.4$$

Sensitivity of the future e^-p collider to the coupling of axion-like particles with W^\pm bosons

- $15 \text{ GeV} \leq m_a \leq 100 \text{ GeV}$

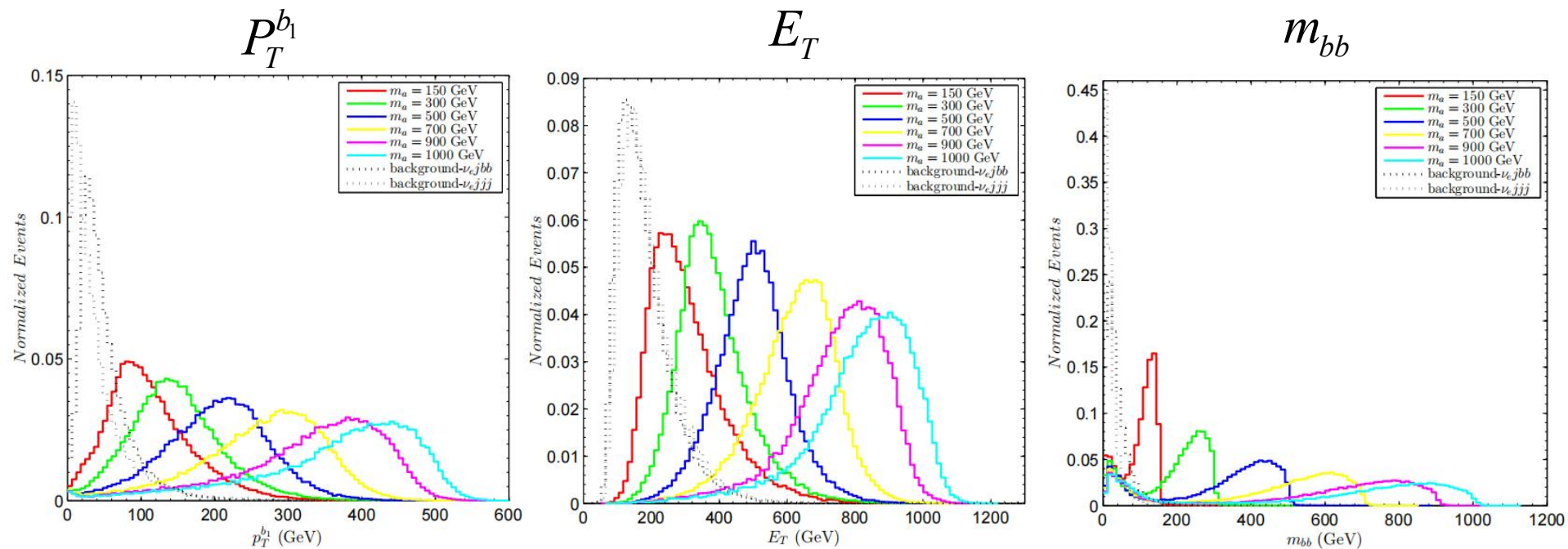


$P_T^{b_1}$



P_T^{bb}

- $100 \text{ GeV} < m_a \leq 1000 \text{ GeV}$





- The improved cuts

Cuts	Mass	
	$15 \text{ GeV} \leq m_a \leq 100 \text{ GeV}$	$100 \text{ GeV} < m_a \leq 1000 \text{ GeV}$
Cut 1	$N_b \geq 2, N_j \geq 1$	$N_b \geq 2, N_j \geq 1$
Cut 2	$m_{bb} > 10 \text{ GeV}$	$p_T^{b_1} > 85 \text{ GeV}$
Cut 3	$p_T^{b_1} > 30 \text{ GeV}$	$E_T > 200 \text{ GeV}$
Cut 4	$\theta_{bb} < 2.9$	$m_{bb} > 100 \text{ GeV}$
Cut 5	$p_T^{bb} > 40 \text{ GeV}$	—

Sensitivity of the future e^-p collider to the coupling of axion-like particles with W^\pm bosons

Cuts	cross sections for signal (background1, background2) [pb]					
	$m_a = 15 \text{ GeV}$	$m_a = 30 \text{ GeV}$	$m_a = 50 \text{ GeV}$	$m_a = 70 \text{ GeV}$	$m_a = 90 \text{ GeV}$	$m_a = 100 \text{ GeV}$
Basic Cuts	6.1000×10^{-5} (0.0490, 6.2968)	1.5831×10^{-3} (0.0490, 6.2968)	2.8332×10^{-3} (0.0490, 6.2968)	3.0975×10^{-3} (0.0490, 6.2968)	3.1289×10^{-3} (0.0490, 6.2968)	3.1248×10^{-3} (0.0490, 6.2968)
Cut 1	2.8250×10^{-5} (0.0271, 0.0922)	8.1835×10^{-4} (0.0271, 0.0922)	1.5797×10^{-3} (0.0271, 0.0922)	1.8036×10^{-3} (0.0271, 0.0922)	1.8604×10^{-3} (0.0271, 0.0922)	1.8691×10^{-3} (0.0271, 0.0922)
Cut 2	2.2980×10^{-5} (0.0231, 0.0576)	7.7615×10^{-4} (0.0231, 0.0576)	1.4986×10^{-3} (0.0231, 0.0576)	1.7120×10^{-3} (0.0231, 0.0576)	1.7665×10^{-3} (0.0231, 0.0576)	1.7751×10^{-3} (0.0231, 0.0576)
Cut 3	1.9960×10^{-5} (0.0177, 0.0387)	7.4325×10^{-4} (0.0177, 0.0387)	1.4409×10^{-3} (0.0177, 0.0387)	1.6500×10^{-3} (0.0177, 0.0387)	1.7096×10^{-3} (0.0177, 0.0387)	1.7228×10^{-3} (0.0177, 0.0387)
Cut 4	1.7110×10^{-5} (9.9450 $\times 10^{-3}$, 0.0250)	6.1904×10^{-4} (9.9450 $\times 10^{-3}$, 0.0250)	1.1660×10^{-3} (9.9450 $\times 10^{-3}$, 0.0250)	1.3126×10^{-3} (9.9450 $\times 10^{-3}$, 0.0250)	1.3244×10^{-3} (9.9450 $\times 10^{-3}$, 0.0250)	1.3193×10^{-3} (9.9450 $\times 10^{-3}$, 0.0250)
Cut 5	1.6290×10^{-5} (8.9469 $\times 10^{-3}$, 0.0220)	6.1644×10^{-4} (8.9469 $\times 10^{-3}$, 0.0220)	1.1534×10^{-3} (8.9469 $\times 10^{-3}$, 0.0220)	1.2712×10^{-3} (8.9469 $\times 10^{-3}$, 0.0220)	1.2725×10^{-3} (8.9469 $\times 10^{-3}$, 0.0220)	1.2629×10^{-3} (8.9469 $\times 10^{-3}$, 0.0220)
SS	0.093	3.468	6.434	7.078	7.084	7.032

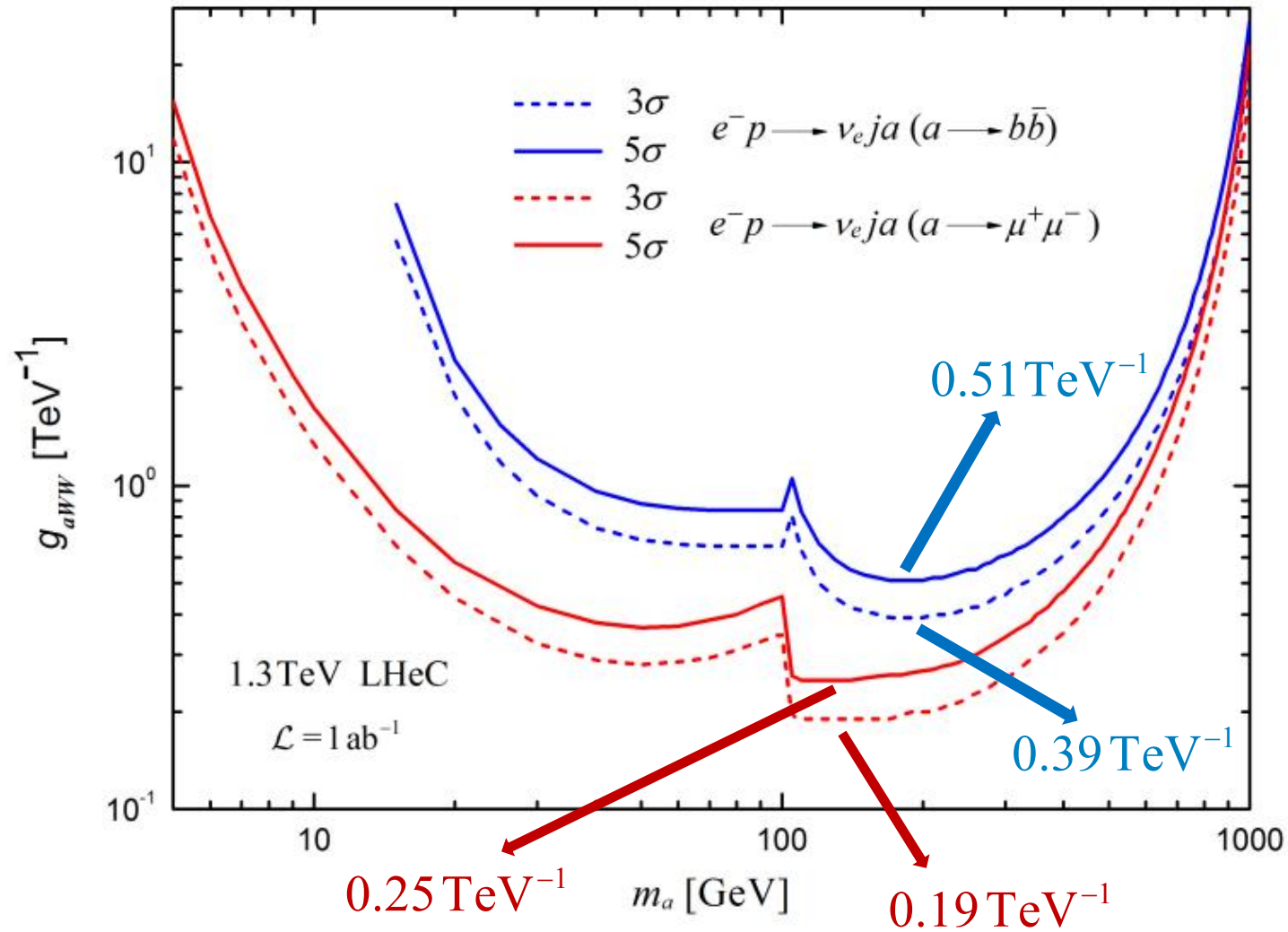
a tagging efficiency of 75% for b jets

a mistagging rate of 5% for c jets

a mistagging rate of 0.1% for other light flavor jets

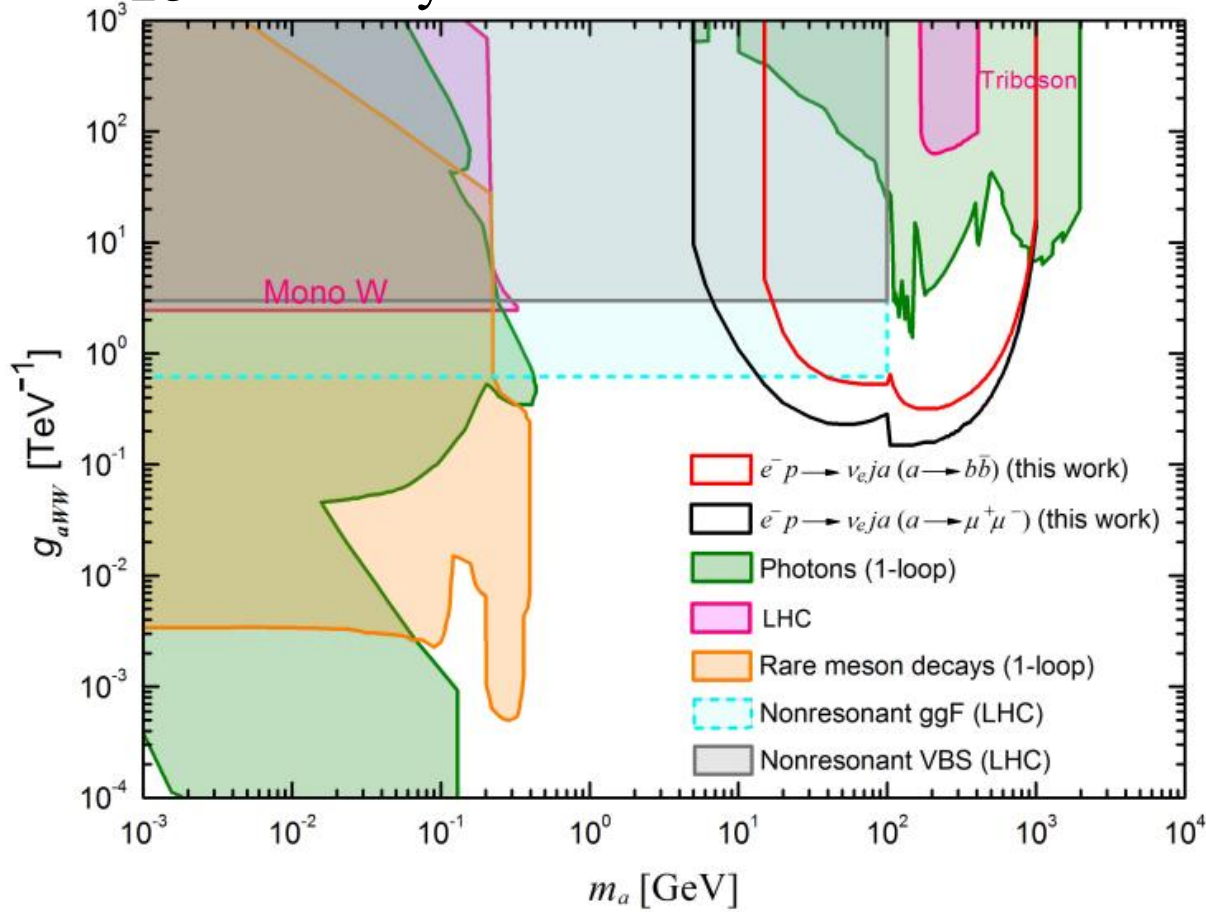
Cuts	cross sections for signal (background1, background2) [pb]					
	$m_a = 150 \text{ GeV}$	$m_a = 300 \text{ GeV}$	$m_a = 500 \text{ GeV}$	$m_a = 700 \text{ GeV}$	$m_a = 900 \text{ GeV}$	$m_a = 1000 \text{ GeV}$
Basic Cuts	2.8355×10^{-3} (0.0490, 6.2968)	1.3969×10^{-3} (0.0490, 6.2968)	3.8331×10^{-4} (0.0490, 6.2968)	6.6391×10^{-5} (0.0490, 6.2968)	4.9981×10^{-6} (0.0490, 6.2968)	7.7509×10^{-7} (0.0490, 6.2968)
Cut 1	1.7067×10^{-3} (0.0271, 0.0922)	8.2443×10^{-4} (0.0271, 0.0922)	2.1850×10^{-4} (0.0271, 0.0922)	3.6355×10^{-5} (0.0271, 0.0922)	2.5790×10^{-6} (0.0271, 0.0922)	3.8905×10^{-7} (0.0271, 0.0922)
Cut 2	1.0934×10^{-3} (3.5966 $\times 10^{-3}$, 9.6278 $\times 10^{-3}$)	6.9825×10^{-4} (3.5966 $\times 10^{-3}$, 9.6278 $\times 10^{-3}$)	2.0489×10^{-4} (3.5966 $\times 10^{-3}$, 9.6278 $\times 10^{-3}$)	3.4825×10^{-5} (3.5966 $\times 10^{-3}$, 9.6278 $\times 10^{-3}$)	2.4991×10^{-6} (3.5966 $\times 10^{-3}$, 9.6278 $\times 10^{-3}$)	3.7804×10^{-7} (3.5966 $\times 10^{-3}$, 9.6278 $\times 10^{-3}$)
Cut 3	1.0447×10^{-3} (2.7793 $\times 10^{-3}$, 7.7577 $\times 10^{-3}$)	6.9545×10^{-4} (2.7793 $\times 10^{-3}$, 7.7577 $\times 10^{-3}$)	2.0480×10^{-4} (2.7793 $\times 10^{-3}$, 7.7577 $\times 10^{-3}$)	3.4825×10^{-5} (2.7793 $\times 10^{-3}$, 7.7577 $\times 10^{-3}$)	2.4991×10^{-6} (2.7793 $\times 10^{-3}$, 7.7577 $\times 10^{-3}$)	3.7804×10^{-7} (2.7793 $\times 10^{-3}$, 7.7577 $\times 10^{-3}$)
Cut 4	7.8474×10^{-4} (8.1555 $\times 10^{-4}$, 8.8780 $\times 10^{-4}$)	5.9819×10^{-4} (8.1555 $\times 10^{-4}$, 8.8780 $\times 10^{-4}$)	1.7398×10^{-4} (8.1555 $\times 10^{-4}$, 8.8780 $\times 10^{-4}$)	2.9176×10^{-5} (8.1555 $\times 10^{-4}$, 8.8780 $\times 10^{-4}$)	2.0992×10^{-6} (8.1555 $\times 10^{-4}$, 8.8780 $\times 10^{-4}$)	3.1304×10^{-7} (8.1555 $\times 10^{-4}$, 8.8780 $\times 10^{-4}$)
SS	15.728	12.461	4.012	0.701	0.050	0.008

• $g_{aWW} = 1 \text{ TeV}^{-1}$



3 Sensitivity of the future e^-p collider to the coupling of axion-like particles with W^\pm bosons

- The projected 2σ sensitivity limits



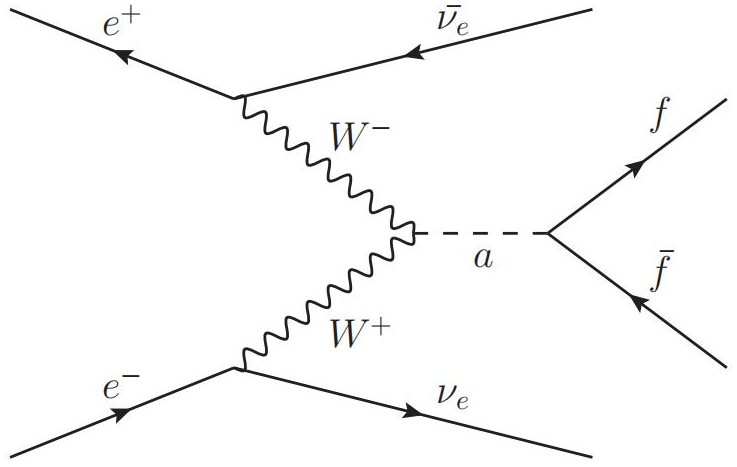
• $e^- p \rightarrow \nu_e j a (a \rightarrow \mu^+ \mu^-) \rightarrow m_a \in [14, 924] \text{ GeV} \quad g_{aWW} \in [0.15, 6.66] \text{ TeV}^{-1}$

• $e^- p \rightarrow \nu_e j a (a \rightarrow b\bar{b}) \rightarrow m_a \in [39, 900] \text{ GeV} \quad g_{aWW} \in [0.32, 6.67] \text{ TeV}^{-1}$



Phys.Lett.B 848 (2024) 138368

Chong-Xing Yue, Han Wang*, Yue-Qi Wang



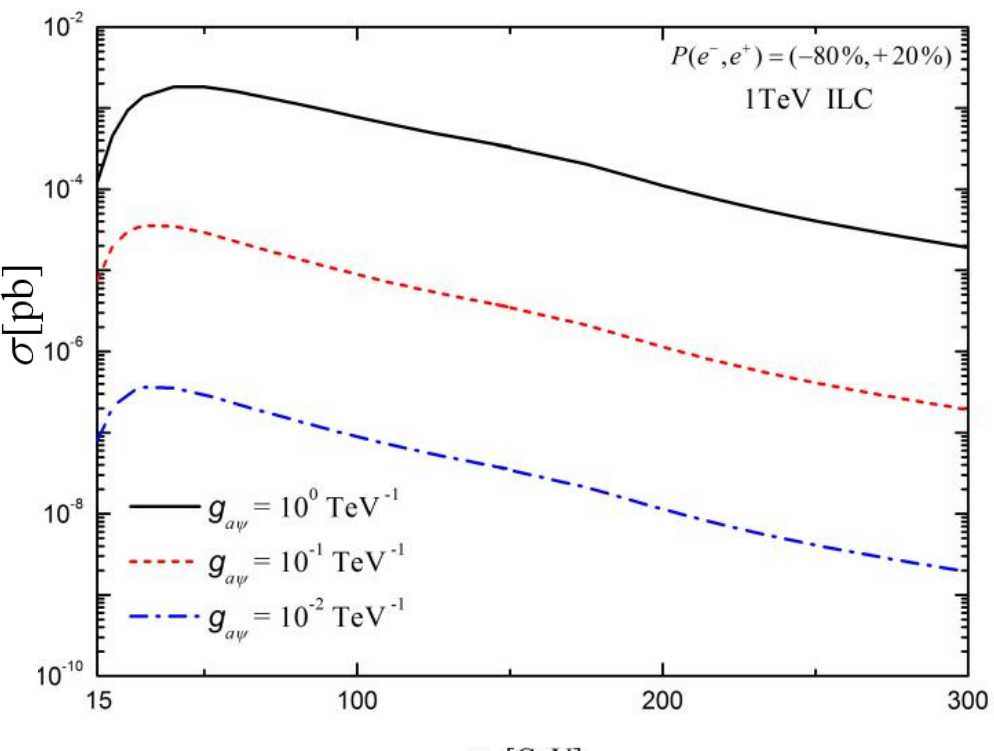
- $\nu_e \bar{\nu}_e t \bar{t} \longrightarrow$ unclean backgrounds

$$m_a < 2 m_t$$

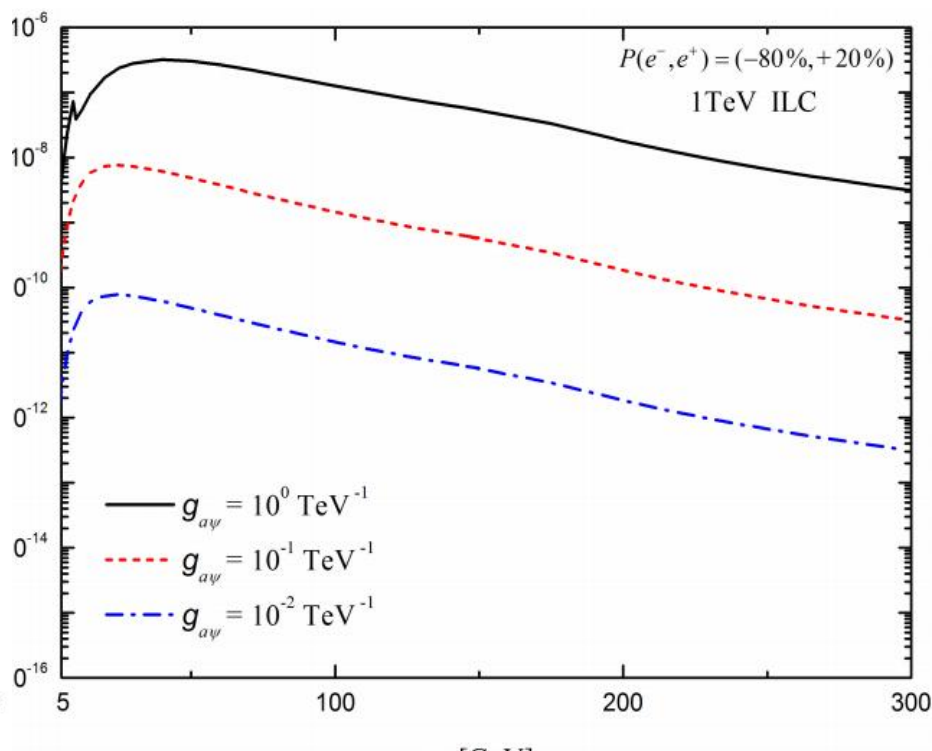
$$\begin{array}{c} \nu_e \bar{\nu}_e c \bar{c} \\ \nu_e \bar{\nu}_e \tau^+ \tau^- \end{array}$$

not tagged efficiently

Detecting the coupling of axion-like particles with fermions at the ILC



$$e^-e^+ \rightarrow \nu_e \bar{\nu}_e a (a \rightarrow b\bar{b})$$



$$e^-e^+ \rightarrow \nu_e \bar{\nu}_e a (a \rightarrow \mu^+\mu^-)$$

- Phys.Rev.D 104 (2021) 9, 092005, 2106.10085



$$g_{aWW} = 0.62 \text{ TeV}^{-1}$$

- ILC

$$E_{CM} = 1 \text{ TeV}$$

$$\mathcal{L} = 1 \text{ ab}^{-1}$$

$$P(e^-, e^+) = (-80\%, +20\%)$$

- Basic cuts:

$$P_T^b > 5 \text{ GeV}$$

$$P_T^l > 20 \text{ GeV}$$

$$|\eta_b| < 2.5 \quad |\eta_j| < 5$$

$$\Delta R_{bb} > 0.4 \quad \Delta R_{jj} > 0.4$$

- $15 \text{ GeV} \leq m_a \leq 50 \text{ GeV}$

the invariant mass m_{bb}

the cone size ΔR_{bb}

the missing transverse energy E_T

the angular separation $\Delta\theta_{bb}$

observables

- $50 \text{ GeV} < m_a \leq 300 \text{ GeV}$

the energy of the hardest b-jet E^{b_1}

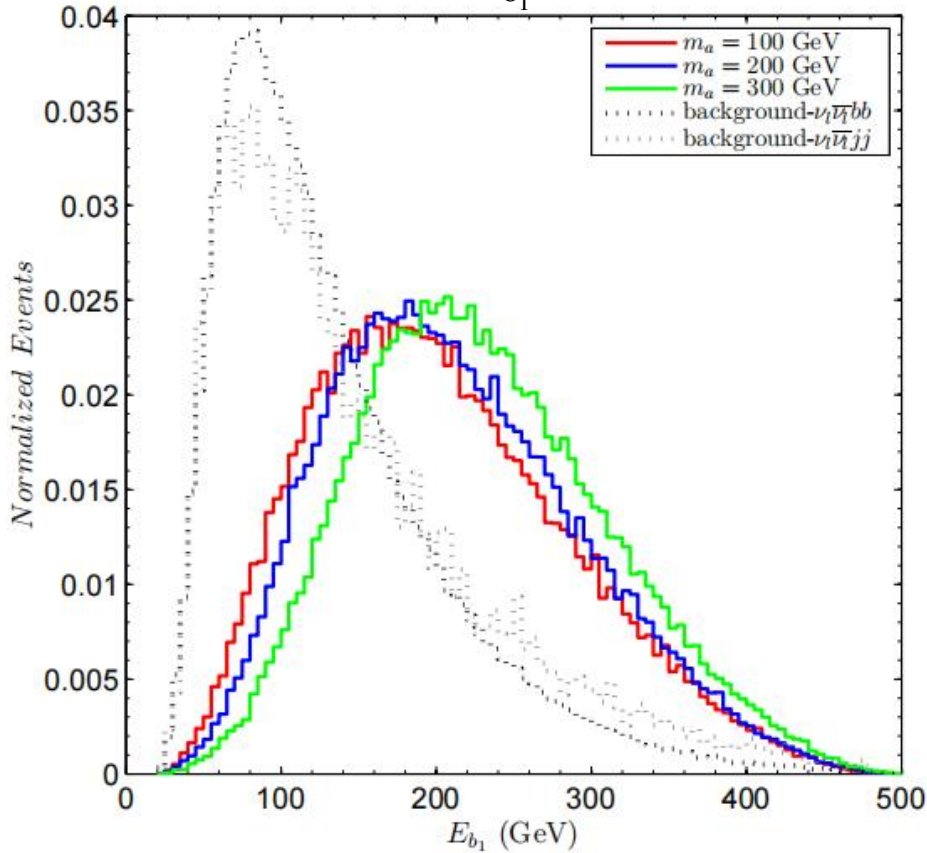
the transverse momentum of the reconstructed ALP P_T^{bb}

observables

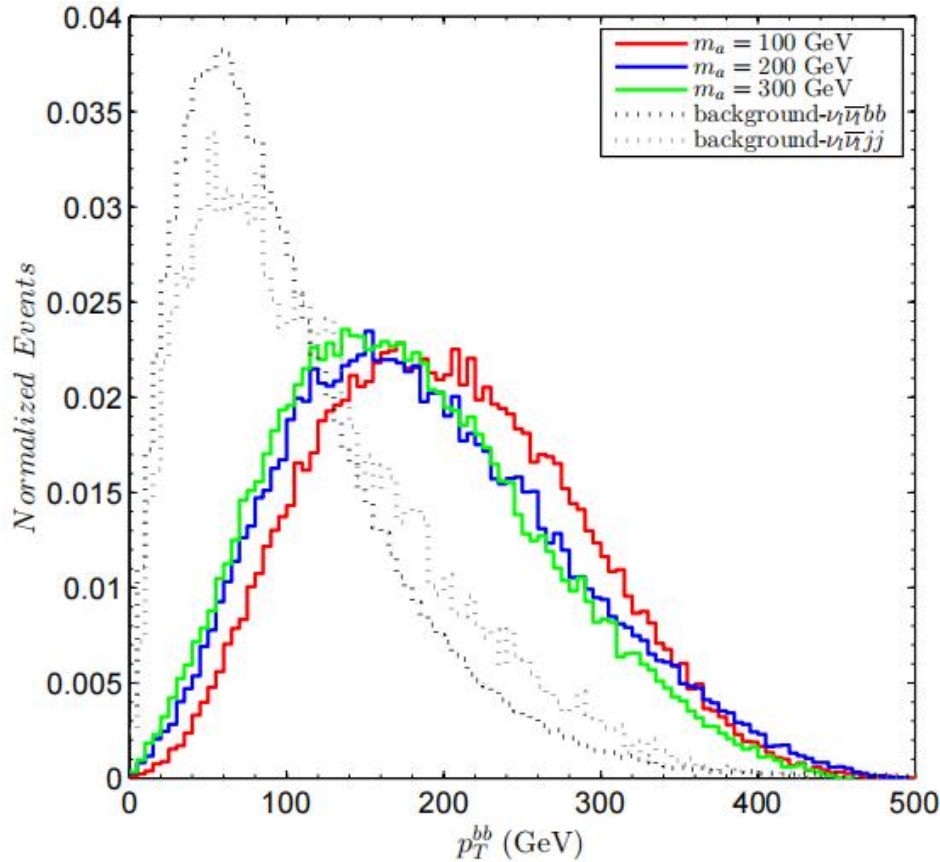
4 Detecting the coupling of axion-like particles with fermions at the ILC

- $50 \text{ GeV} < m_a \leq 300 \text{ GeV}$

E_{b_1}



P_T^{bb}





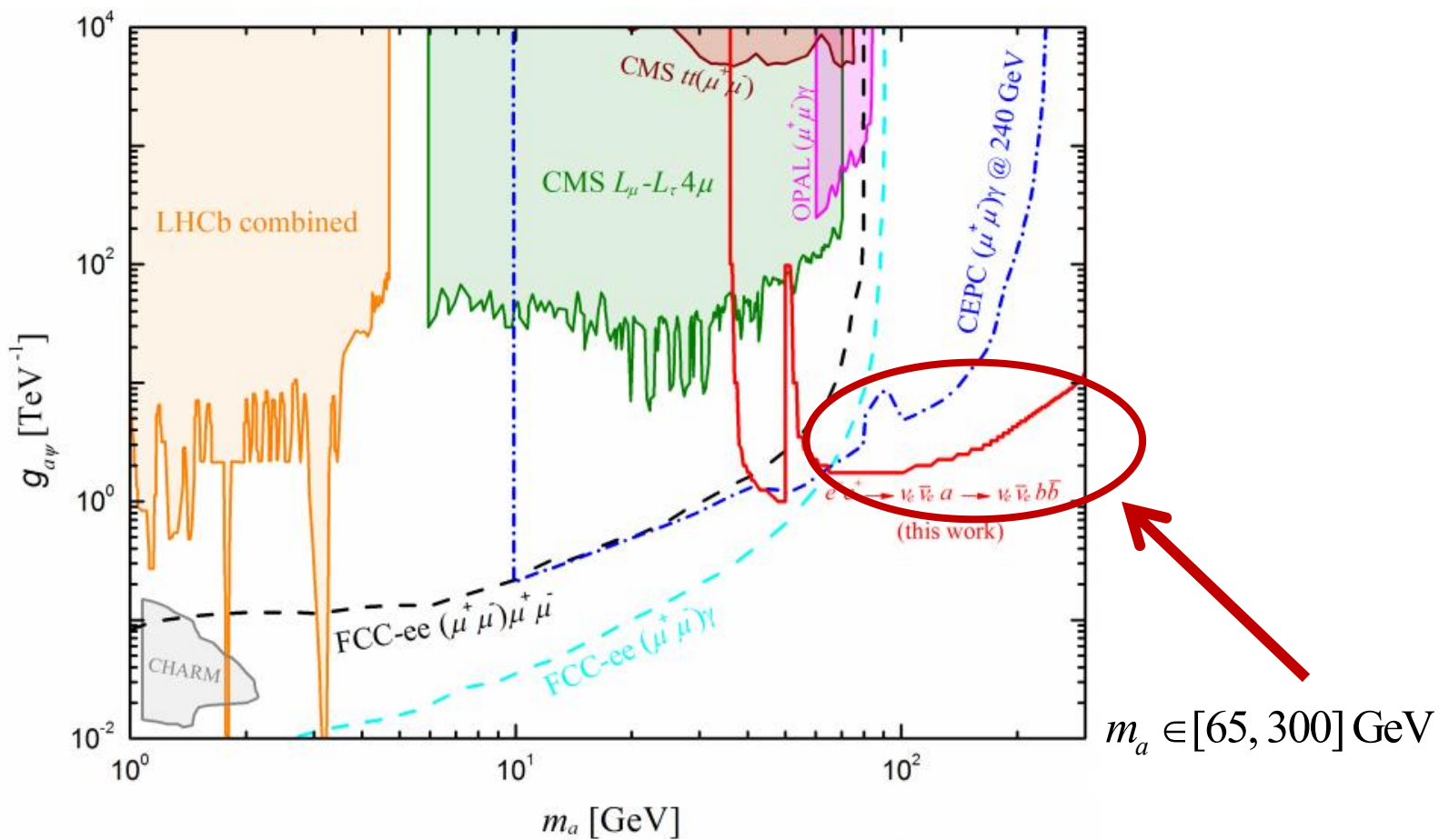
- The improved cuts

Cuts	Mass	
	$15 \text{ GeV} \leq m_a \leq 50 \text{ GeV}$	$50 \text{ GeV} < m_a \leq 300 \text{ GeV}$
Cut 1	$N_b \geq 2$	$N_b \geq 2$
Cut 2	$m_{bb} < 80 \text{ GeV}$	$E_{b_1} > 120 \text{ GeV}$
Cut 3	$\Delta R_{bb} < 1$	$p_T^{bb} > 100 \text{ GeV}$
Cut 4	$\cancel{E}_T > 40 \text{ GeV}$	—
Cut 5	$\Delta\theta_{bb} < 0.8$	—

4 Detecting the coupling of axion-like particles with fermions at the ILC

Cuts	Cross sections for signal ($bg-\nu_l\bar{\nu}_l b\bar{b}$, $bg-\nu_l\bar{\nu}_l jj$) [pb]		
	$m_a = 100 \text{ GeV}$	$m_a = 200 \text{ GeV}$	$m_a = 300 \text{ GeV}$
Basic Cuts	5.4310×10^{-3} (0.6889, 0.8857)	3.1891×10^{-3} (0.6889, 0.8857)	1.0866×10^{-3} (0.6889, 0.8857)
Cut 1	1.6686×10^{-3} (0.1809, 4.3155×10^{-3})	1.3018×10^{-3} (0.1809, 4.3155×10^{-3})	4.9840×10^{-4} (0.1809, 4.3155×10^{-3})
Cut 2	1.3973×10^{-3} (0.0835, 2.1934×10^{-3})	1.1422×10^{-3} (0.0835, 2.1934×10^{-3})	4.6240×10^{-4} (0.0835, 2.1934×10^{-3})
Cut 3	1.3170×10^{-3} (0.0535, 1.6275×10^{-3})	1.0191×10^{-3} (0.0535, 1.6275×10^{-3})	3.9370×10^{-4} (0.0535, 1.6275×10^{-3})
SS	5.545	4.300	1.671

- $g_{a\Psi} = 10 \text{ TeV}^{-1}$



- $m_a \in [37, 50]$ GeV $\longrightarrow g_{a\psi} \rightarrow 1$ TeV $^{-1}$
- $m_a \in [52, 300]$ GeV $\longrightarrow g_{a\psi} \rightarrow 1.75$ TeV $^{-1}$

5 Conclusions



- ALP appears naturally in broad extensions of the SM, which have various beneficial properties to search by many high energy experiments
- The promising sensitivities of the 240 GeV CEPC to the coupling $g_{a\gamma\gamma}$ are in the range of 0.0325TeV^{-1} to 0.037TeV^{-1} with m_a from 2.9 GeV to 190 GeV
- The 1.3 TeV LHeC is more sensitive to the coupling g_{aWW} via the W^+W^- fusion processes $e^- p \rightarrow \nu_e ja(a \rightarrow \mu^+ \mu^-)$ and $e^- p \rightarrow \nu_e ja(a \rightarrow b\bar{b})$ for ALP with the mass range of roughly a few tens to 900 GeV
- The currently unconstrained $m_a - g_{a\Psi}$ parameter space can be covered by the 1 TeV ILC, for which the corresponding reaches are 1TeV^{-1} and 1.75TeV^{-1} from $37 \text{GeV} \leq m_a \leq 50 \text{GeV}$ and $52 \text{GeV} \leq m_a \leq 300 \text{GeV}$, respectively



物理与电子技术学院
School of Physics and Electronic
Technology, LNU



遼寧師範大學
Liaoning Normal University



Searching for axion-like particles at future e^+e^- and e^-p colliders

Thanks

Han Wang (王晗)

Liaoning Normal University

27th Mini-workshop on the frontier of LHC

2024.01.22